ACS APPLIED MATERIALS & INTERFACES

Research Article

www.acsami.org

Highly Flexible, Proton-Conductive Silicate Glass Electrolytes for Medium-Temperature/Low-Humidity Proton Exchange Membrane Fuel Cells

Hyeon-Ji Lee,[†] Jung-Hwan Kim,[†] Ji-Hye Won,[‡] Jun-Muk Lim,[‡] Young Taik Hong,*[,§] and Sang-Young Lee*[,†]

[†]Interdisciplinary School of Green Energy, Ulsan National Institute of Science and Technology (UNIST), Ulsan, 689-798, Korea

[‡]Department of Chemical Engineering, College of Engineering, Kangwon National University, Chuncheon, Kangwondo, 200-701, Korea

[§]Energy Materials Research Center, Korea Research Institute of Chemical Technology, Daejeon 305-600, Korea

ABSTRACT: We demonstrate highly flexible, proton-conductive silicate glass electrolytes integrated with polyimide (PI) nonwoven fabrics (referred to as "b-SS glass electrolytes") for potential use in medium-temperature/low-humidity proton exchange membrane fuel cells (PEMFCs). The b-SS glass electrolytes are fabricated via in situ sol−gel synthesis of 3-trihydroxysilyl-1-propanesulfonic acid (THPSA)/3-glycidyloxypropyl trimethoxysilane (GPTMS) mixtures inside PI nonwoven substrates that serve as a porous reinforcing framework. Owing to this structural uniqueness, the b-SS glass electrolytes provide noticeable improvements in mechanical bendability and membrane thickness, in comparison to typical bulk silicate glass electrolytes that are thick and easily fragile. Another salient feature of the b-SS glass electrolytes is the excellent proton conductivity at harsh measurement conditions of medium temperature/low humidity, which is highly important for PEMFC-powered electric vehicle applications. This beneficial performance is attributed to the presence of a highly interconnected, proton-conductive (THPSA/GPTMS-based) silicate glass matrix in the PI reinforcing framework. Notably, the b-SS glass electrolyte synthesized from THPSA/GPTMS = 9/1 (mol/mol) exhibits a higher proton conductivity than water-swollen sulfonated polymer electrolyte membranes (here, sulfonated poly(arylene ether sulfone) and Nafion are chosen as control samples). This intriguing behavior in the proton conductivity of the b-SS glass electrolytes is discussed in great detail by considering its structural novelty and Grotthuss mechanism-driven proton migration that is strongly affected by ion exchange capacity (IEC) values and also state of water.

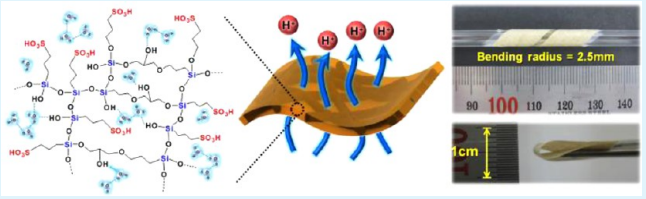

KEYWORDS: *PEMFCs, flexible silicate glass electrolytes, polyimide nonwoven fabrics, THPSA/GPTMS, proton conductivity, medium-temperature/low-humidity*

1. INTRODUCTION

Recently, proton exchange membrane fuel cells (PEMFCs) have garnered increasing attention as an environmentally friendly and efficient energy conversion system, particularly for applications in electric vehicles and residential energy supplies.[1−3] Among various components of PEMFCs, a proton exchange membrane is considered a key element that significantly affects electrochemical performance of PEMFCs because it acts as a proton-conductive electrolyte, gas barrier, and electronic separator membrane between electrodes.[4−6] Over the past few decades, water-swollen polymer electrolytes bearing sulfonic acid groups (e.g., perfluorosulfonic acid polymers (including Nafion) and sulfonated hydrocarbon copolymers) have been extensively investigated as one of the most popular proton exchange membranes. Notably, from the viewpoint of practical application to PEMFCs, these hydrated polymer electrolytes show many advantageous characteristics such as high proton conductivity, film-forming capability, mechanical toughness, and electrochemical stability.

Meanwhile, as the scientific/industrial importance of PEMFC-powered electric vehicles (PEMFC-EVs), which are spotlighted as a next-generation clean transportation system, is rapidly growing, advanced proton exchange membranes capable of imparting satisfactory electrochemical performance (in particular, proton conductivity) at medium-temperature (above 80 °C)/low-humidity conditions are strongly demanded. Unfortunately, when the above-mentioned water-swollen polymer electrolytes are exposed to these harsh operating conditions, they tend to be easily dehumidified, and consequently their hydration-dependent proton conductivity is significantly impaired.[4−8]

One drastic approach to resolve this stringent drawback of hydrated polymer electrolytes is the development of sol−gel-derived proton-conductive glass electrolytes, which are

Received: March 6, 2013
Accepted: May 14, 2013
Published: May 14, 2013

Scheme 1. Schematic Representations Depicting the Overall Fabrication Procedure and Unique Morphology of b-SS Glass Electrolyte, Wherein Conceptual Pathways for Proton Transport and Chemical Structure of the Three-Dimensionally Interconnected SS Glass Matrix Are Also Illustrated

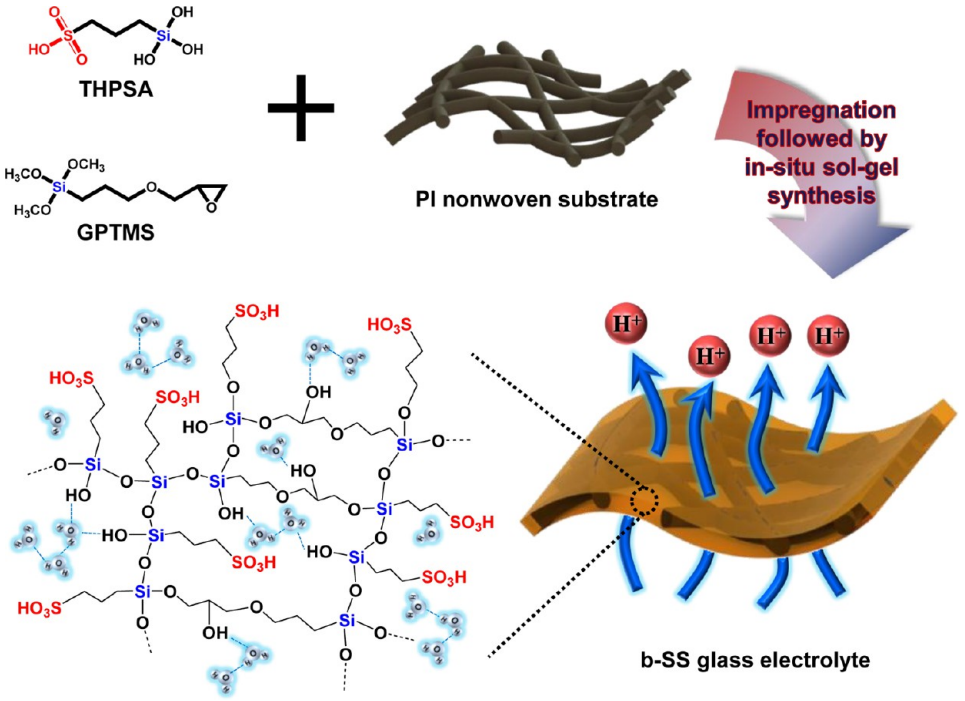

generally composed of silicate glass networks and mixed acid species. These silicate glass electrolytes are featured with the electrochemical stability, potentially cost competitiveness, and, more importantly, excellent proton conductivity at dehumidified conditions.[9−17] Representative examples of the silicate glass electrolytes are described below. Lu et al.[13] fabricated phosphonic acid-modified silicas using co-condensation of diethylphosphatoethyl triethoxysilane and tetraethoxysilane (TEOS). The silica electrolytes exhibited the high proton conductivity of 4.4×10^{-4} S cm^{-1} at 150 °C/20% relative humidity (RH). Tung et al.[14,15] proposed a new sol−gel process for SiO_2−P_2O_5 glass electrolytes by controlling water/vapor composition ratio. Nogami et al.[16] reported P_2O_5−TiO_2−SiO_2 ternary glass electrolytes aimed at low-humidity applications. Yogo et al.[17] reported proton-conductive inorganic−organic hybrid electrolytes from 3-glycidyloxypropyl trimethoxysilane (GPTMS) and various hydroxyl alkyl phosphonic acids, which showed high proton conductivity of 10^{-4} S cm^{-1} at 130 °C/dehumidified conditions.

Although these silicate glass electrolytes afford high proton conductivity at dehumidified conditions, they still confront formidable challenges in securing a satisfactory level of mechanical flexibility and membrane thickness because of their intrinsically brittle and fragile nature. In an effort to improve the mechanical flexibility of silicate glass electrolytes, Li et al.[18] demonstrated a multilayer-structured polyethylenimine-poly(*o*-creslglycidylether)-co-formaldehyde (as an organic layer)/phosphosilicate (as an inorganic layer) membrane. The brittle inorganic phosphosilicate layer was mechanically supported by the organic layer; however, the presence of the organic layer having relatively poor proton conductivity led to unsatisfactory proton conductivity of ∼10^{-5} S cm^{-1} at 70 °C/90% RH.

Meanwhile, reinforced composite membranes consisting of mechanically reinforcing porous substrates and proton-conductive electrolytes have drawn considerable interest owing to their excellence in membrane thickness, mechanical strength, and dimensional stability.[19−21] As part of ongoing research to develop advanced reinforced composite membranes, our group has recently explored the feasibility of polyimide (PI) nonwovens as a new reinforcing porous substrate.[22−24]

In the present study, encouraged by the successful fabrication of PI nonwoven-reinforced composite membranes, we demonstrate highly flexible, proton-conductive silicate glass electrolytes (hereinafter, referred to as "b-SS glass electrolytes") as a new architectural strategy to develop innovative proton exchange membranes. The b-SS glass electrolyte proposed herein is fabricated via in situ sol−gel synthesis of a 3-trihydroxysilyl-1-propanesulfonic acid (THPSA)/GPTMS mixture inside a PI nonwoven substrate. This leads to the formation of a highly interconnected matrix of sulfonic acid-functionalized silicate glass (hereinafter, referred to as "SS glass") electrolyte, serving as effective proton-conductive channels, in the PI nonwoven substrate. Here, the PI nonwoven substrate, which is produced from electrospun PI nanofibers,[22−24] is incorporated as a reinforcing framework to impart mechanical flexibility and toughness.

Owing to this structural uniqueness, the b-SS glass electrolyte is expected to provide significant improvements in mechanical bendability and membrane thickness, as compared to typical bulk silicate glass electrolytes that are thick and easily fragile. In addition, the THPSA containing sulfonic acid groups covalently bonded to silicon atoms through alkylene groups enables the resulting SS glass matrix to tightly hold water molecules and thus to afford excellent proton conductivity at dehumidified conditions.[25,26] The GPTMS with epoxy ring and flexible

dx.doi.org/10.1021/am400836h | ACS Appl. Mater. Interfaces 2013, 5, 5034−5043

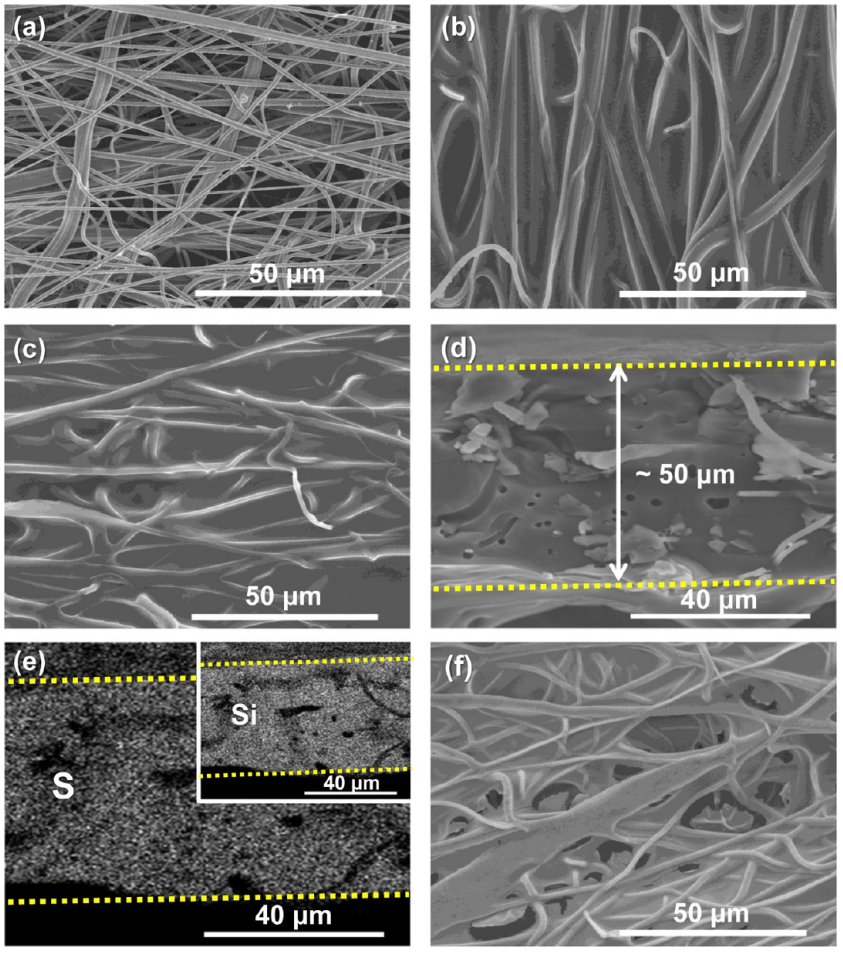

Figure 1. FE-SEM photographs (surface) of: (a) pristine PI nonwoven fabric; (b) b-SS glass electrolyte (THPSA/GPTMS = 5/5); (c) b-SS glass electrolyte (THPSA/GPTMS = 9/1). FE-SEM photographs (cross-section) of (d) b-SS glass electrolyte (THPSA/GPTMS = 9/1); (e) EDS images of b-SS glass electrolyte (THPSA/GPTMS = 9/1), wherein the bright dots signify the S and Si elements of the impregnated SS glass matrix. (f) A control sample (THPSA/GPTMS = 10/0).

organic chain (i.e., glycidoxypropyl group) is employed as a mechanical softening linker to prevent the crack formation during the sol−gel synthesis. Hence, it should be noted that the physical properties and electrochemical performance (in particular, proton conductivity) of the SS glass electrolyte are strongly dependent on the composition ratio of THPSA/GPTMS mixtures.

Herein, structural/physical properties of the b-SS glass electrolytes, including morphology, chemical structure, mechanical bendability, and dimensional stability, are systematically investigated. On the basis of this characterization, the potential application of the b-SS glass electrolytes (as a new proton-conductive membrane) to medium-temperature/low-humidity PEMFCs is explored by scrutinizing proton conductivity at various measurement conditions, and the results are compared with those of a sulfonated polymer electrolyte membrane. Here, the sulfonated polymer electrolytes are chosen as a control system, reflecting their popularity in commercial PEMFCs for recently spotlighted EV applications. As a representative example of the sulfonated polymer electrolytes, sulfonated poly(arylene ether sulfone) (SPAES), in addition to Nafion, is selected owing to its high ionic conductivity, good electrochemical performance, and low-cost synthesis.[6,24,26]

Another noteworthy advantage of the b-SS glass electrolytes, in addition to their excellent mechanical bendability and membrane thickness, is the provision of higher proton conductivity than the water-swollen sulfonated polymer electrolyte membranes at harsh measurement conditions of medium temperature/low RH. This intriguing behavior in proton conductivity of the b-SS glass electrolyte is discussed with an in-depth consideration of its structural novelty and Grotthuss mechanism-driven proton migration that is strongly influenced by ion exchange capacity (IEC) values and state of water.

2. EXPERIMENTAL SECTION

2.1. Fabrication of Proton-Conductive Silicate Glass Electrolytes Integrated with Polyimide Nonwoven Fabrics (b-SS Glass Electrolytes). A coating solution for the fabrication of sulfonic acid-functionalized silicate glass (SS glass) was prepared by mechanically mixing THPSA (FluoroChem), GPTMS (Aldrich), and 0.1 N HNO_3 in dimethylacetamide (DMAc) as a solvent for 1 h at 60 °C, wherein the mole-based composition ratio of THPSA/GPTMS mixtures was, respectively, varied as 5/5, 7/3, and 9/1. Electrospun PI nonwoven fabrics (KFM-NT, average thickness ~40 ± 2 μm, average porosity ~80%) were provided from Kolon (Korea). The aforementioned coating solution was directly applied to the PI nonwoven via a dip-coating process. The coating solution-immersed PI nonwoven was dried at room temperature for 2 h and then subjected to stepwise thermal treatment (50 → 100 → 120 → 140 °C, for 4 h at each

temperature) in a hot oven for completing the sol−gel reaction.[24] Finally, a self-standing b-SS glass electrolyte (average thickness ∼50 μm) was obtained. A schematic representation illustrating the overall fabrication procedure (i.e., the impregnation of THPSA/GPTMS mixtures into the PI nonwoven fabrics followed by the in situ sol−gel synthesis), along with chemical structure and unusual architecture of the b-SS glass electrolyte, is shown in Scheme 1.

Meanwhile, a pristine SPAES membrane was prepared as a control sample by casting 10 wt % SPAES solution onto a glass plate. The SPAES (degree of sulfonation = 50%) was synthesized via nucleophilic aromatic substitution polymerization of 4,4′-dichlorodiphenylsulfone, 3,3′-disulfonated 4,4′-dichlorodiphenylsulfone, and 4,4′-biphenol. The detailed synthesis of the SPAES has been described in previous publications.[6,7,27] The Nafion membrane, another control sample, was fabricated by casting Nafion DE521 solution (5 wt %, EW 1100, DuPont) onto a glass plate followed by drying at 80 °C for 3 h. The thickness of the SPAES and Nafion membrane was approximately 60 μm.

2.2. Characterization of Proton-Conductive Silicate Glass Electrolytes Integrated with Polyimide Nonwoven Fabrics (b-SS Glass Electrolytes). The morphological characterization of the b-SS glass electrolytes was carried out using a field emission resolution scanning electron microscope (FE-SEM, S-4800, Hitachi) equipped with an energy-dispersive spectrometer (EDS). The chemical structure of the b-SS glass electrolytes was elucidated by a FT-IR spectrometer (FT-3000, BIO-RAD) with a spectral resolution of 4 cm^{-1}. The X-ray powder diffraction (XRD) patterns of the b-SS glass electrolytes were obtained on a PANalytical diffractometer using Cu Kα radiation (λ = 0.1541 nm), where the data were collected from 10 to 50 (2θ) with a resolution of 0.02°. The mechanical bendability of the b-SS glass electrolytes was evaluated from a bending cycle test using a universal tensile tester (Lloyd LR10K, Lloyd Instruments), where samples were subjected to a repeated bending stress until being mechanically ruptured, at a strain rate of 50 mm min^{-1}.[28] Here, the number of bending cycles before breakdown of the samples quantitatively represents their mechanical bendability. To measure the dimensional change (i.e., area-based dimensional expansion/shrinkage) of membranes with varying humidity, the membranes were placed in an oven at 25 °C/95% RH for 6 h. The samples were then dried in a vacuum oven at 100 °C for 12 h. The area of the samples was estimated before (A_{wet}) and after (A_{dry}) the vacuum drying step. The change in the area (ΔA) of the samples was estimated using the equation ΔA (%) = $[(A_{wet} - A_{dry})/A_{dry}] \times 100$.[22−24] The ion exchange capacity (IEC) values of the membranes were quantitatively measured using a conventional titration method (ASTM D2187).[14] The in-plane proton conductivities of the membranes were evaluated with an impedance analyzer (VSP classic, Bio-Logic) using a four-probe method over a frequency range of 1×10^{-1} to 2×10^{5} Hz,[24] where the sample dimension is 3 cm × 1 cm (width × length). For the proton conductivity measurement, the samples were pre-equilibrated in a temperature/humidity control chamber (SH-241, ESPEC) under a given condition of temperature and RH. Meanwhile, the state of water in the membranes was examined by a thermogravimetric analyzer (TGA, SDT Q600, TA Instruments).[22,23] The TGA experiment was performed in a temperature range from room temperature (isothermal heating at 100 °C for 40 min was inserted to ensure the evaporation of physically adsorbed water) to 400 °C at a heating rate of 10 °C min^{-1} under a nitrogen atmosphere. Prior to the TGA measurement, the membranes were placed in an oven at 30 °C/95% RH for 4 h and then pre-equilibrated at 30 °C/50% RH for 2 h. The fraction of physically adsorbed water was quantified by measuring the weight loss below 100 °C. The amount of chemically adsorbed water was obtained by subtracting the physically adsorbed water content from the total water content. To evaluate the total water content in the membranes, the membranes preequilibrated at 30 °C/50% RH for 2 h were vacuum-dried at 100 °C for 24 h. The total water content (ΔW (wt %) = $[(W_{wet} - W_{dry})/W_{dry}] \times 100$) was estimated by measuring the weight difference of the samples before and after the vacuum drying step.[22,23]

3. RESULTS AND DISCUSSION

3.1. Structural/Compositional Uniqueness and Mechanical Bendability of b-SS Glass Electrolytes. The structural/compositional uniqueness of the b-SS glass electrolytes was investigated by carrying out FE-SEM, FT-IR, and XRD characterization. Figure 1a shows that the PI nonwoven fabric is composed of multifibrous layers possessing large-sized pores (approximately more than 10 μm) formed between the microdiameter fibers. A distinctive morphological feature of the b-SS glass electrolytes is the integration of PI reinforcing framework with SS glass matrix. For all the b-SS glass electrolytes examined herein, the PI nonwoven substrate is well-impregnated with the SS glass matrix (THPSA/GPTMS = 5/5 (Figure 1b) and 9/1 (Figure 1c)). This unusual structure of the b-SS glass electrolytes is further confirmed by observing the cross-sectional morphology (Figure 1d) and EDS images (Figure 1e), where the b-SS glass electrolyte (THPSA/GPTMS = 9/1) was chosen as a representative sample. In particular, the EDS images exhibit that the bright dots signifying the S and Si elements assigned to the sulfonic acid group and silicate skeleton of the SS glass are uniformly dispersed in the thickness direction of the b-SS glass electrolyte.

It is known that proton conductivity of a porous substrate-reinforced composite membrane strongly depends on the porous structure of a reinforcing substrate because the reinforcing substrate is electrochemically inert to proton transport.[19−24] In other words, interconnectivity and amount of impregnated proton-conductive electrolytes play crucial roles in determining the proton conductivity of reinforced composite membranes. The morphological results shown in Figure 1 demonstrate that the highly developed porous structure (average porosity ∼80%) of the PI nonwoven substrate beneficially contributes to the formation of a three-dimensionally interconnected SS glass matrix in the b-SS glass electrolyte. As a result, this morphological uniqueness of the b-SS glass electrolyte is expected to exert a positive influence on the construction of favorable pathways for facile proton transport, which is conceptually illustrated in Scheme 1. More details on the proton transport behavior of b-SS glass electrolytes will be discussed in the following sections.

Meanwhile, as a control experiment, THPSA solution (without GPTMS) was solely applied to the PI nonwoven substrate. In contrast to the b-SS glass electrolytes fabricated from the THPSA/GPTMS mixtures, the resulting composite electrolyte shows a number of large-scale cracks (Figure 1f) because the THPSA-based silicates tend to be mechanically brittle and insufficient to accommodate volume change occurring during the sol−gel synthesis.[29,30] This result demonstrates that the combination of THPSA with GPTMS bearing the glycidoxypropyl groups (i.e., functional epoxy rings and flexible organic chains), followed by the in situ sol−gel synthesis, is an effective way to successfully fabricate crack- (or defect-) free silicate glass electrolytes directly inside the PI nonwoven substrate.

Another notable advantage of the b-SS glass electrolyte is the low membrane thickness (∼ 50 μm), which is quantitatively shown in Figure 1d. Typical bulk silicate glass electrolytes are known to generally have a thickness of more than a few hundred micrometers.[9−17] Moreover, due to their fragile and brittle attributes, reducing the membrane thickness remains a formidable challenge. In this respect, the incorporation of PI reinforcing framework into the b-SS glass electrolyte can be

suggested as a promising route to overcome the stringent limitation of bulk silicate glass electrolytes.

The chemical structure of the b-SS glass electrolyte was elucidated by analyzing the FT-IR peaks, where the b-SS glass electrolyte (THPSA/GPTMS = 9/1) was chosen as a representative example. Meanwhile, the FT-IR peaks of the PI nonwoven substrate and bulk SS glass electrolyte (without PI nonwoven substrate) were also characterized as control samples. Figure 2a shows that a strong absorption peak (~1028 cm^{-1}, denoted as <1>) assigned to the vibration of Si−O−Si bonds[10,13] is found at the b-SS glass electrolyte as well as the bulk SS glass electrolyte. This indicates that, during the in situ sol−gel synthesis directly conducted in the PI nonwoven substrate, the SiO_2 networks comprising Si−O−Si linkages are successfully formed in the SS glass matrix of the b-SS glass electrolyte. Another characteristic peak (~1125 cm^{-1}, denoted as <2>) ascribed to the S−O stretching is found at the b-SS glass electrolyte and also the bulk SS glass electrolyte, which confirms the presence of the SS glass matrix bearing SO_3H groups in the PI−GC membrane.[25] The typical stretching vibration of CH_2 units is observed at around 2875 cm^{-1} (denoted as <3>), verifying that the SS glass matrix of the b-SS glass electrolyte is synthesized from the GPTMS.[17] In hygroscopic silicate glass electrolytes, water molecules are known to readily establish hydrogen bonding with Si−OH groups. The broad absorption band at 3360 cm^{-1} (denoted as <4>), corresponding to stretching vibrations of Si−O−H involved in the hydrogen bonding with adsorbed water molecules,[10,12,15] indicates the construction of hydrogen bonding networks in the b-SS glass electrolyte. This hydrogen bonding formed between the SS glass matrix and water molecules is conceptually illustrated in Scheme 1. Intriguingly, the FT-IR characterization, along with the previous morphological result (Figure 1), confirms the presence of the PI reinforcing framework in the b-SS glass electrolyte. The characteristic FT-IR peak (~ 1707 cm^{-1}, denoted as <5>) ascribed to the C═O bonds of the imide ring[31] is found at the PI nonwoven substrate and also the b-SS glass electrolyte.

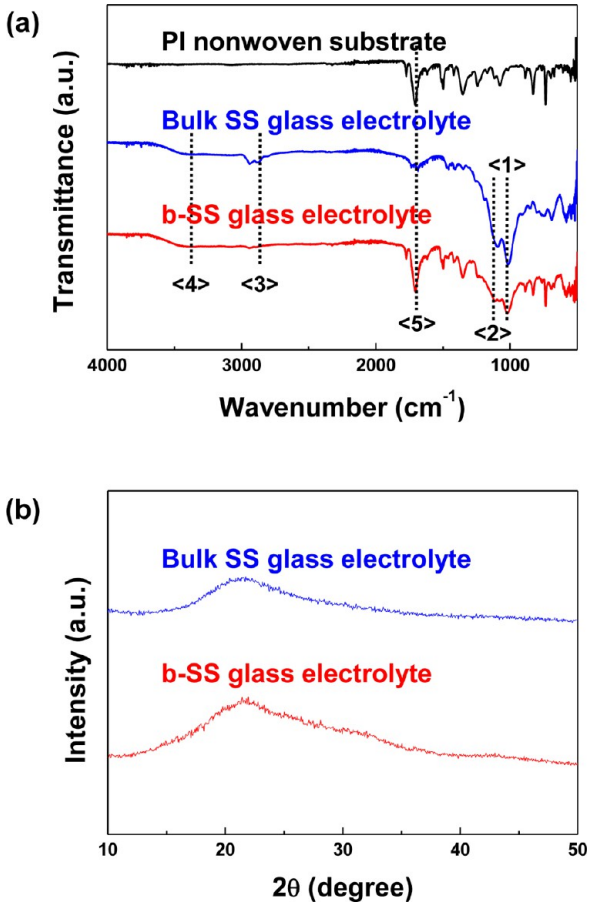

Figure 2. (a) FT-IR spectra of PI nonwoven substrate, bulk SS glass electrolyte, and b-SS glass electrolyte: Si−O−Si linkage (denoted as <1>), S−O groups (denoted as <2>), CH_2 units (denoted as <3>), Si−O−H involved in the hydrogen bonding with adsorbed water molecules (denoted as <4>), and C═O bonds of the imide ring (denoted as <5>). (b) XRD spectra of bulk SS glass electrolyte and b-SS glass electrolyte.

The XRD pattern of the b-SS glass electrolyte (THPSA/GPTMS = 9/1) was examined and compared with that of the bulk SS glass electrolyte (Figure 2b). In both electrolytes, a reflection peak assigned to typical amorphous silicate glass is observed at around 20°.[12,16] This reveals that, similar to the bulk SS glass electrolyte, the SS glass matrix of the b-SS glass electrolyte has no long-range order of crystalline phase. Notably, it is observed that the difference in XRD patterns between the bulk SS glass electrolyte and b-SS glass electrolyte is inappreciable. This XRD analysis, in addition to the previous FT-IR result, demonstrates that the chemical structure and amorphous phase of the SS glass matrix in the b-SS glass electrolyte are not impaired by the incorporation of the PI reinforcing framework.

The mechanical flexibility of the b-SS glass electrolyte (THPSA/GPTMS = 9/1) was examined and compared with that of the bulk SS glass electrolyte incorporating no PI reinforcing framework. Figure 3 shows that the b-SS glass electrolyte and bulk SS glass electrolyte are opaque, brownish, and self-standing under a static state. When these glass electrolytes are subjected to bending stress, the bulk SS glass electrolyte is easily broken down (Figure 3a). By contrast, the b-SS glass electrolyte is highly bendable (bending radius = 2.5 mm) and twistable. Moreover, no mechanical rupture is observed after being folded at a bending angle of almost 180° (Figure 3b). The superior bendability of the b-SS glass electrolyte was further examined using a bending cycle test, where the number of bending cycles (under longitudinal strain ranged from 1 to 3 cm) before breakdown of the samples quantitatively represents their mechanical bendability.[28] Figure 3c shows that the b-SS glass electrolyte has a strong tolerance to mechanical breakage upon appreciable bending stress and retains its dimensional stability even after the 100th bending cycle. More notably, micrometer-scaled structural stability of the SS glass matrix in the b-SS glass electrolyte is well-preserved even after the bending cycle test (Figure 3d). This drastic improvement in the mechanical bendability underlines that the introduction of the compliant PI nonwoven substrate as a mechanically reinforcing framework is an effective approach to overcoming the formidable limitation of intrinsically brittle silicate glass electrolytes.

The dimensional change (i.e., area-based dimensional expansion/shrinkage) of the b-SS glass electrolyte (THPSA/GPTMS = 9/1) with varying humidity was compared with that of the hydrated SPAES and Nafion membrane, before/after being dehumidified in a vacuum oven (25 °C/95% RH → 100 °C/vacuum). It is shown in Figure 4 that the dimensional change (ΔA) of the SPAES membrane and Nafion membrane

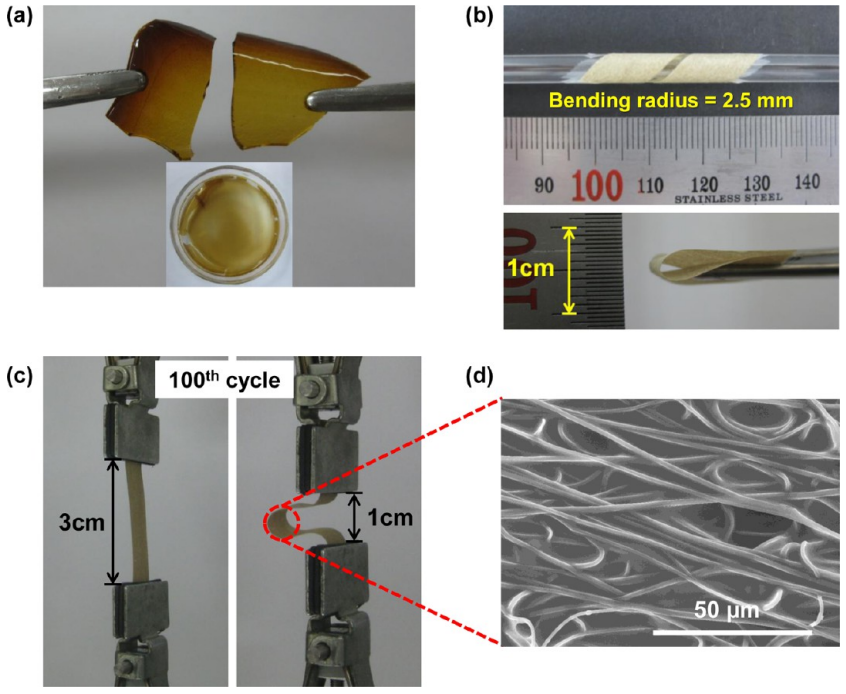

Figure 3. Photographs showing mechanical flexibility of glass electrolytes: (a) bulk SS glass electrolyte; (b) b-SS glass electrolyte after being subjected to various types of bending deformation; (c) b-SS glass electrolyte after being subjected to the 100th bending cycle, where a strain rate was 50 mm min^{-1}. (d) A FE-SEM photograph demonstrating the structural stability of the b-SS glass electrolyte after the 100th bending cycle.

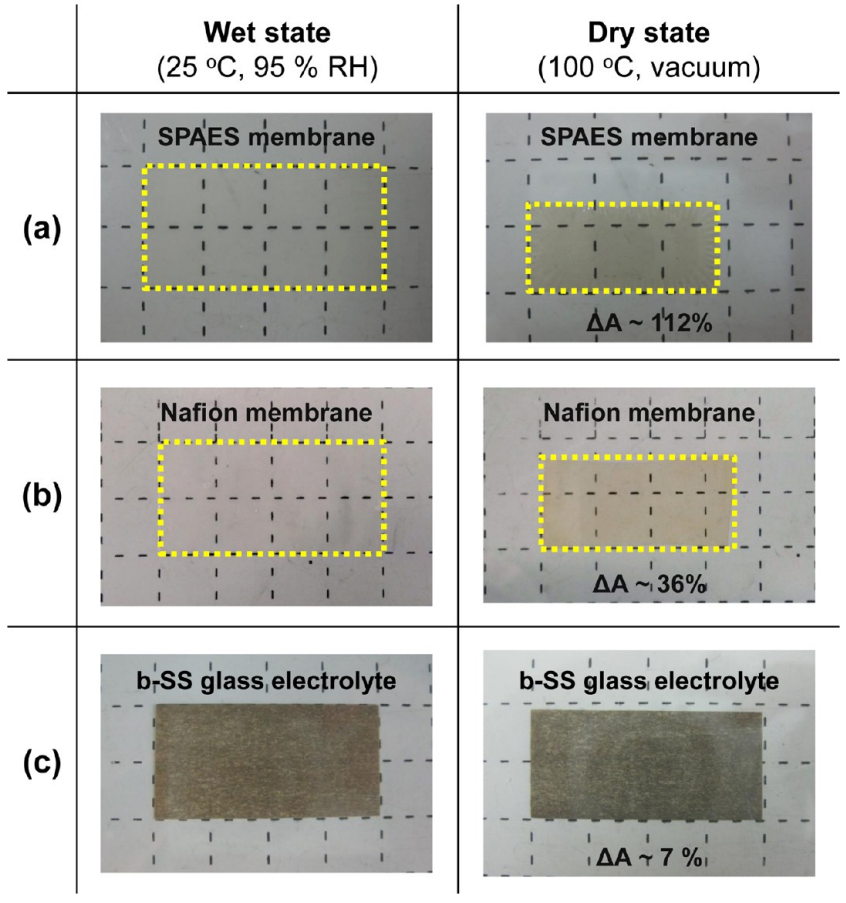

Figure 4. Comparison of dimensional change between (a) SPAES membrane; (b) Nafion membrane; and (c) b-SS glass electrolyte (THPSA/GPTMS = 9/1), where the (area-based) dimensional change (ΔA) of the membranes was estimated using the equation ΔA (%) = $[(A_{wet} - A_{dry})/A_{dry}] \times 100$.

dx.doi.org/10.1021/am400836h | ACS Appl. Mater. Interfaces 2013, 5, 5034−5043

is, respectively, ∼112% and ∼36%. In conventional water-swollen sulfonated polymer electrolytes, their dimensional stability is strongly dependent on degree of hydration. Hence, high degree of hydration could give rise to large swelling of polymer chains, leading to large area expansion of the water-swollen membranes. On the other hand, the dimensional change of the b-SS glass electrolyte is found to be negligibly small ($\Delta A \sim 7\%$). The aforementioned morphological characterization exhibited that the SS glass electrolyte is composed of the SS glass matrix and the PI nonwoven substrate. This structural uniqueness enables the b-SS glass electrolyte to have strong resistance against the humidity variation-driven dimensional deformation, as compared to water-swollen polymer electrolytes.

3.2. Temperature-/RH-Dependent Proton Conductivity of b-SS Glass Electrolytes for Potential Application to Medium-Temperature/Low-Humidity PEMFCs. On the basis of the above-mentioned structural/mechanical characterization of the b-SS glass electrolytes, their temperature-/RH-dependent proton conductivity was scrutinized as a function of THPSA/GPTMS composition ratio in the SS glass matrix. Unfortunately, the proton transport behavior of the bulk SS glass electrolyte incorporating no PI nonwoven substrate (i.e., bulk SS glass electrolyte having the same chemical structure and composition as those of the SS glass matrix in the b-SS glass electrolyte) was difficult to characterize, as the bulk SS glass electrolyte was too brittle and fragile to be manipulated for proton conductivity measurement.

First, the IEC values of the b-SS glass electrolytes were estimated using a titration method.[25] Table 1 shows that the b-SS glass electrolytes provide the higher IEC values as the THPSA content in the SS glass matrix is increased. It has been previously observed that the SS glass matrix is fabricated inside the PI reinforcing framework via in situ sol−gel synthesis of THPSA bearing sulfonic acid (SO_3H) groups and ionically nonconductive GPTMS. Therefore, the incorporation of larger THPSA content is expected to raise the IEC values of the SS glass matrix. The variation in the IEC values of the b-SS glass electrolytes was further confirmed by measuring their proton conductivity (here, at 80 °C/80% RH). Table 1 exhibits that, as the IEC value of the b-SS glass electrolyte is increased from 1.26 (THPSA/GPTMS = 5/5) to 2.47 mmol g^{-1} (THPSA/GPTMS = 9/1), its proton conductivity becomes more enhanced (0.014 → 0.166 S cm^{-1}). Notably, the b-SS glass electrolyte (THPSA/GPTMS = 9/1) shows a higher proton conductivity (= 0.166 S cm^{-1}) than the SPAES (= 0.037 S cm^{-1}) and Nafion (= 0.070 S cm^{-1}) membranes, which is well-consistent with its higher IEC value.

Table 1. Summary of IEC Values and Proton Conductivity (At a Condition of 80 °C/80% RH) of b-SS Glass Electrolytes, SPAES Membrane, and Nafion Membrane, Where IEC Values Were Measured Using a Conventional Titration Method (ASTM D2187)

sample		ion exchange capacity [IEC, mmol g^{-1}]	proton conductivity [σ, S cm^{-1}]
b-SS glass electrolyte	THPSA/GPTMS = 5/5	1.26 ± 0.10	0.014
	THPSA/GPTMS = 7/3	1.83 ± 0.08	0.063
	THPSA/GPTMS = 9/1	2.47 ± 0.11	0.166
SPAES membrane		1.56 ± 0.09	0.037
Nafion membrane		1.03 ± 0.07	0.070

Figure 5a shows the temperature-dependent proton conductivity of the b-SS glass electrolytes at 60% RH. For all the b-SS glass electrolytes, their proton conductivities tend to increase as the temperature rises from 30 to 70 °C. This is attributed to the boosted mobility of hydrated protons at higher temperatures. Meanwhile, consistent with the aforementioned IEC results, the proton conductivity of the b-SS glass electrolytes tends to be improved at all measurement temperatures as the THPSA content in the SS glass matrix is increased. This interesting behavior of proton conductivity is further verified by estimating activation energy for proton conduction. The activation energy for proton conduction was observed to be 43.34 (THPSA/GPTMS = 5/5) to 26.93 kJ mol^{-1} (THPSA/GPTMS = 9/1), which verifies that the larger THPSA content (i.e., higher concentration of sulfonic acid groups) is beneficial in lowering activation energy for ionic migration. This strong dependency of the proton transport on the THPSA/GPTMS composition ratio is conceptually illustrated in Figure 5b. Another noteworthy finding is that the b-SS glass electrolyte (THPSA/GPTMS = 9/1) shows a higher proton conductivity than the SPAES and Nafion membranes over a wide range of temperatures, demonstrating its promising potential as a new proton-conductive electrolyte to outperform conventional hydrated polymer electrolytes.

As a next step, to explore the applicability of b-SS glass electrolytes to PEMFCs (particularly, targeting PEMFC-EV applications), their proton conductivities were investigated at harsh measurement conditions such as medium temperature/low RH. The proton conductivities of the b-SS glass electrolytes were evaluated as a function of RH at 80 °C (Figure 6a). In accordance with our expectations, the proton conductivities of the electrolytes are gradually deteriorated as the RH is decreased from 80 to 50%. This reveals that the proton conductivity is strongly affected by membrane dehydration. Interestingly, the b-SS glass electrolyte (THPSA/GPTMS = 9/1) exhibits a higher proton conductivity than the SPAES and Nafion membrane over a wide range of RHs. Under these dehumidified conditions, the SPAES and Nafion membranes are easily dehydrated, resulting in a considerable loss of the proton conductivity. It is known that the proton conductivity of water-swollen sulfonated polymer electrolyte membranes such as SPAES and the Nafion membrane is strongly dependent on their degree of hydration.[6,7,27] The previous FT-IR results (Figure 2a) showed that the hydroxyl and sulfonic acid groups exist in the SS glass matrix of the b-SS glass electrolyte. These polar groups may allow the b-SS glass electrolyte to have strong affinity for water molecules and good water retention at dehumidified conditions. Therefore, it is expected that, at low RH conditions, a relatively larger amount of strongly adsorbed water molecules can be engaged in the proton transport of the b-SS glass electrolyte, thereby contributing to the higher proton conductivity. More detailed discussion based on the understanding of state of water in the b-SS glass electrolytes will be presented in the following section.

The proton conductivities of the b-SS glass electrolytes were further examined at more challenging measurement conditions (above 100 °C/dry-out states). Figure 6b shows that the proton conductivity of the SPAES membrane falls sharply with increasing temperature, disclosing that the membrane is significantly dehydrated at these harsh conditions. A notable finding is that, for the b-SS glass electrolytes, the decline in the proton conductivity is highly retarded. For example, at a

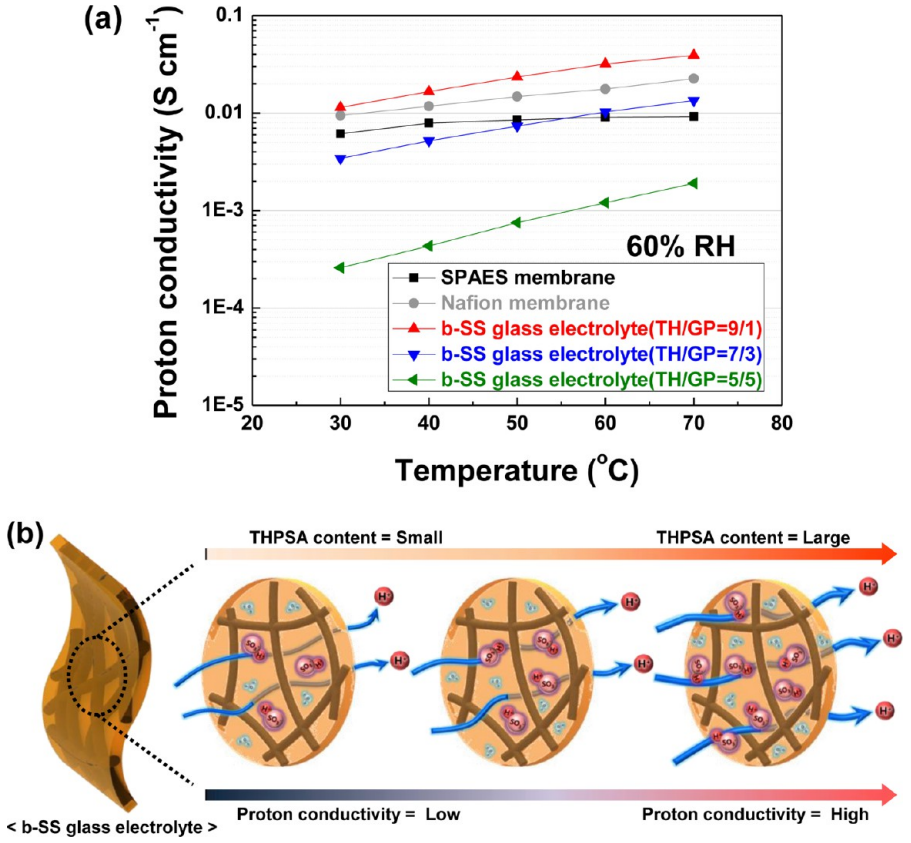

Figure 5. (a) Temperature-dependent proton conductivities of SPAES membrane, Nafion membrane, and b-SS glass electrolytes at 60% RH. (b) A schematic illustration explaining proton transport of b-SS glass electrolyte as a function of THPSA/GPTMS composition ratio in SS glass matrix.

condition of 120 °C/dry-out state, the proton conductivity ($\sigma \sim 0.01$ S cm^{-1}) of the b-SS glass electrolyte (THPSA/GPTMS = 9/1) is found to be more than 1 order of magnitude higher than that ($\sigma \sim 0.0003$ S cm^{-1}) of the SPAES membrane.

At these extremely dehumidified conditions, the b-SS glass electrolyte is expected to tightly hold water molecules owing to the presence of polar groups (i.e., hydroxyl and sulfonic acid groups) of the SS glass matrix. In addition, the b-SS glass electrolyte (THPSA/GPTMS = 9/1) has a larger amount of sulfonic acid groups (reflected from the higher IEC values) than other b-SS glass electrolytes due to the presence of larger THPSA content. As a result, the distance between two neighboring sulfonic acid groups may be shortened, thereby boosting up the rate of proton transport. This densely populated sulfonic acid group of the b-SS glass electrolyte (THPSA/GPTMS = 9/1), in conjunction with its strong water retention capability, could exert a beneficial effect on Grotthuss mechanism-driven proton migration.[4−6,10−12]

To provide a better understanding of the unusual proton conductivity at dehumidified conditions, an in-depth investigation of the state of water in the b-SS glass electrolytes was conducted. It has been previously reported[22,23] that the state of water in proton-conducting electrolytes could be classified into two groups from an analysis of TGA thermograms: physically adsorbed water (i.e., free and slightly bound water) and chemically adsorbed water (i.e., strongly bound water). Here, the weight loss below 100 °C is ascribed to vaporization of physically adsorbed water in membranes, and the weight loss above 100 °C (= total water content in membranes − the weight loss below 100 °C) is attributed to desorption of chemically adsorbed water. Meanwhile, considering the cautionary remark on the quantitative use of thermodynamic data for interpreting the state of water,[32] it should be noted that the TGA thermogram-based analysis of water molecules is restricted to conducting a relative comparison between the samples, rather than delivering the absolute value of the state of water.

Figure 7a depicts the weight loss profiles of water molecules for the b-SS glass electrolytes with varied composition ratio of THPSA/GPTMS and hydrated sulfonated polymer electrolyte membranes (i.e., SPAES and Nafion) as a function of temperature, where isothermal heating of 100 °C/40 min was additionally introduced to secure sufficient time for evaporation of physically adsorbed water.[22,23] From these TGA profiles, the physically adsorbed water and chemically adsorbed water in the total water content were quantitatively evaluated. Figure 7b shows that the total water contents are 16.0 wt % (SPAES membrane), 5.7 wt % (Nafion membrane), 23.5 wt % for the b-SS glass electrolyte (THPSA/GPTMS = 9/1), 12.0 wt % for the b-SS glass electrolyte (THPSA/GPTMS = 7/3), and 6.9 wt % for the b-SS glass electrolyte (THPSA/GPTMS = 5/5), respectively. In particular, when the b-SS glass electrolytes are concerned as a function of THPSA/GPTMS composition ratio, it is apparent that the total water contents tend to decrease as the THPSA/GPTMS ratio is decreased, which is consistent with the aforementioned results of IEC values and proton conductivity.

The water molecules held in the hydrated sulfonated polymer electrolyte membranes and also b-SS glass electrolytes are more scrutinized in Figure 7b, in terms of the state of water (i.e., physically adsorbed water and chemically adsorbed water). Overall behavior in the state of water appears to be well-

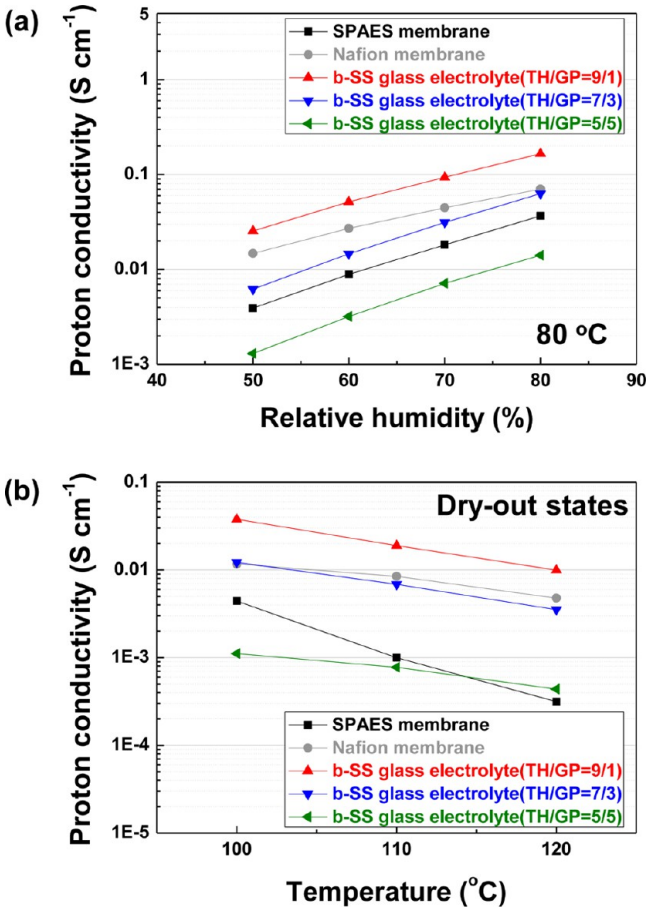

Figure 6. (a) RH-dependent proton conductivities of the SPAES membrane, Nafion membrane, and b-SS glass electrolytes at 80 °C. (b) Temperature-dependent proton conductivities of the SPAES membrane, Nafion membrane, and b-SS glass electrolytes at high-temperature (above 100 °C)/dry-out states.

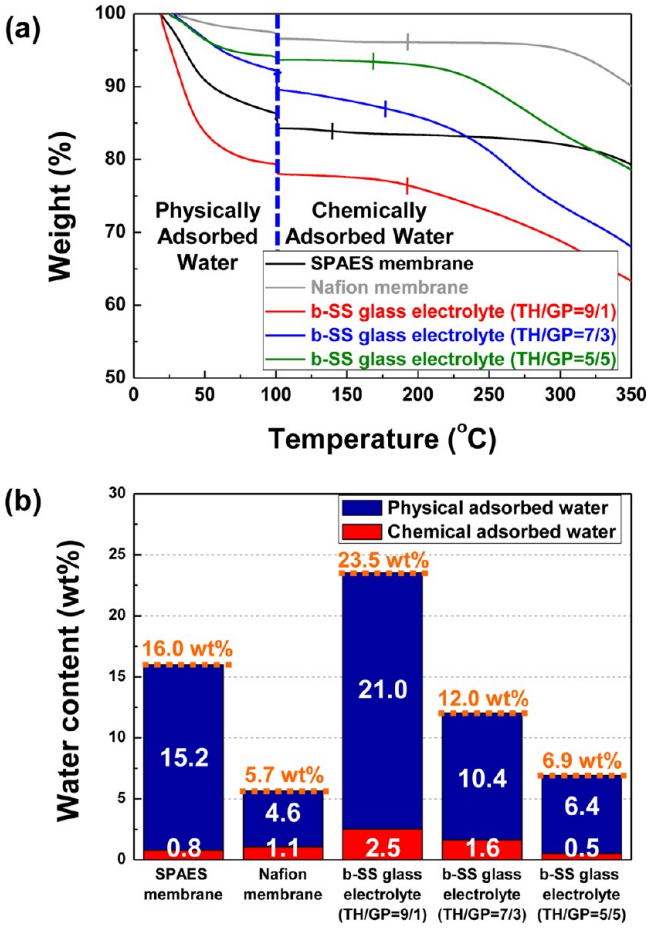

Figure 7. Characterization of state of water for SPAES membrane, Nafion membrane, and b-SS glass electrolytes: (a) TGA thermograms at a heating rate of 10 °C min^{-1}, wherein an isothermal heating of 100 °C/40 min was additionally introduced to allow sufficient time for evaporation of physically adsorbed water and (b) analysis of physically adsorbed water and chemically adsorbed water in the total water content of the samples.

consistent with the results of total water contents. Here, focusing on the SPAES membrane and b-SS glass electrolyte (THPSA/GPTMS = 9/1) as representative samples, an in-depth discussion about the relationship between the state of water and proton conductivity is described. For the SPAES membrane, the weight loss corresponding to physically adsorbed water is 15.2 wt %, and the weight loss ascribed to chemically adsorbed water is 0.8 wt %. On the other hand, in the b-SS glass electrolyte (THPSA/GPTMS = 9/1), the weight loss for physically adsorbed water is 21.0 wt %, and the weight loss for chemically adsorbed water is 2.5 wt %. This result confirms that the b-SS glass electrolyte holds a larger amount of water molecules than the SPAES membrane due to the presence of a hygroscopic SS glass matrix imparting high concentration of hydroxyl and sulfonic acid groups. More importantly, the larger amount of chemically adsorbed water in the b-SS glass electrolyte could be solid evidence to explain the superior proton conductivity at the harsh measurement conditions of above 100 °C/dry-out states (Figure 6b). It is known that, at dehumidified conditions, the contribution of chemically adsorbed water to proton transport of membranes becomes more influential.[22−24,33] A conceptual representation illustrating the presence of chemically adsorbed water molecules, which strongly adhere to the SS glass matrix of b-SS glass electrolyte via hydrogen bonding, is presented in Scheme 1.

4. CONCLUSION

The highly flexible, proton-conductive silicate glass electrolyte integrated with the PI nonwoven fabric (b-SS glass electrolyte) has been developed for potential use in medium-temperature/low-humidity PEMFCs. The in-depth structural/compositional characterization exhibited that the sulfonic acid-functionalized silicate glass (SS glass) matrix, serving as highly interconnected proton-conductive channels, was successfully formed inside the PI porous reinforcing framework via the in situ sol−gel synthesis of THPSA/GPTMS mixtures. Due to this unique architectural feature, the b-SS glass electrolyte provided significant improvement in the mechanical bendability (notably, no mechanical rupture even after being subjected to repeated bending stress) and membrane thickness, as compared to typical bulk silicate glass electrolytes that are thick and easily fragile. Another remarkable benefit of the b-SS glass electrolyte was the excellent proton conductivity at harsh measurement conditions of medium temperature/low RH, which was strongly dependent on the composition ratio of THPSA/GPTMS mixtures in the SS glass matrix. Notably, the b-SS glass electrolyte (THPSA/GPTMS = 9/1) showed the higher proton conductivity than the hydrated sulfonated polymer electrolyte membranes such as SPAES and Nafion. This superior proton

conductivity of the b-SS glass electrolyte at dehumidified conditions was interpreted by considering the densely populated sulfonic acid groups (verified from the higher IEC values) and larger amount of chemically adsorbed water (estimated from the TGA analysis), both of which were expected to facilitate Grotthuss mechanism-driven proton migration. Our subsequent studies will be devoted to further improvement of proton conductivity and mechanical properties of reinforcing framework-integrated silicate glass electrolytes by fine-tuning their chemical structure, composition ratio, and functional groups, which will be followed by electrochemical characterization of membrane−electrode assemblies (MEAs) incorporating the composite glass electrolytes. We believe that the structural engineering proposed herein, i.e., the exquisite combination of a silicate glass electrolyte with a PI nonwoven fabric, offers an attractive route toward the fabrication of flexible proton-conductive glass membranes with desirable attributes and functionality.

AUTHOR INFORMATION

Corresponding Author

*E-mail: ythong@krict.re.kr. Tel.: +82 42 860 7292. Fax: +82 42 860 7237 (Young Taik Hong). E-mail: syleek@unist.ac.kr. Tel.: +82 52 217 2948. Fax: +82 52 217 2019 (Sang-Young Lee).

Notes

The authors declare no competing financial interest.

ACKNOWLEDGMENTS

This work was supported by the National Research Foundation of Korea Grant funded by the Korean Government (MEST) (NRF-2012-M1A2A2-029542). This research was also supported by the Converging Research Center Program through the Ministry of Education, Science and Technology (2012K001254). This research has also been performed as a cooperation project of the KRICT OWN Project and supported by the Korea Research Institute of Chemical Technology (KRICT). The authors are grateful to Prof. Hoi Ri Moon at UNIST for her kind assistance with TGA measurement.

REFERENCES

(1) Devanathan, R. *Energy Environ. Sci.* **2008**, *1*, 101−119.
(2) Buratto, S. K. *Nat. Nanotechnol.* **2010**, *5*, 176.
(3) Peighambardoust, S. J.; Rowshanzamir, S.; Amjadi, M. *Int. J. Hydrogen Energy* **2010**, *35*, 9349−9384.
(4) Mauritz, K. A.; Moore, R. B. *Chem. Rev.* **2004**, *104*, 4535−4585.
(5) Kreuer, K. D. *J. Membr. Sci.* **2001**, *185*, 29−39.
(6) Hickner, M. A.; Ghassemi, H.; Kim, Y. S.; Einsla, B. R.; McGrath, J. E. *Chem. Rev.* **2004**, *104*, 4587−4612.
(7) Erdinc, O.; Uzunoglu, M. *Renewable Sustainable Energy Rev.* **2010**, *14*, 2874−2884.
(8) Thiam, H. S.; Daud, W. R. W.; Kamarudin, S. K.; Mohammad, A. B.; Kadhum, A. A. H.; Loh, K. S.; Majlan, E. H. *Int. J. Hydrogen Energy* **2011**, *36*, 3187−3205.
(9) Jiang, F.; Di, Z.; Tu, H.; Yu, Q.; Li, H. *J. Power Sources* **2011**, *196*, 1048−1054.
(10) Jin, D.; Kong, X.; Tu, H.; Yu, Q.; Jiang, F.; Li, H. *Microporous Mesoporous Mater.* **2011**, *138*, 63−67.
(11) Yoshida, H.; Matsuda, A.; Minami, T.; Tatsumisago, M.; Tadanaga, K. *Electrochim. Acta* **2004**, *50*, 705−708.
(12) Li, H.; Jin, D.; Yu, Q.; Tu, H. *J. Power Sources* **2011**, *196*, 3836−3840.
(13) Jin, Y. G.; Qiao, S. Z.; Xu, Z. P.; Yan, Z.; Huang, Y.; Costa, J. C. D.; Lu, G. Q. *J. Mater. Chem.* **2009**, *19*, 2363−2372.
(14) Tung, S. P.; Hwang, B. J. *J. Mater. Chem.* **2005**, *15*, 3532−3538.
(15) Tung, S. P.; Hwang, B. J. *J. Membr. Sci.* **2004**, *241*, 315−323.
(16) Uma, T.; Izuhara, S.; Nogami, M. *J. Eur. Ceram. Soc.* **2006**, *26*, 2365−2372.
(17) Umeda, J.; Moriya, M.; Sakamoto, W.; Yogo, T. *J. Membr. Sci.* **2009**, *326*, 701−707.
(18) Li, H.; Ai, M.; Jiang, F.; Tu, H.; Yu, Q. *Solid State Ionics* **2011**, *190*, 25−29.
(19) Wang, L.; Yi, B. L.; Zhang, H. M.; Liu, Y. H.; Xing, D. M.; Shao, Z. G.; Cai, Y. H. *J. Power Sources* **2007**, *167*, 47−52.
(20) Rodgers, M. P.; Berring, J.; Holdcroft, S.; Shi, Z. *J. Membr. Sci.* **2008**, *321*, 100−113.
(21) Tang, H.; Pan, M.; Wang, F.; Shen, P. K.; Jiang, S. P. *J. Phys. Chem. B* **2007**, *111*, 8684−8690.
(22) Lee, J. R.; Kim, N. Y.; Lee, M. S.; Lee, S. Y. *J. Membr. Sci.* **2011**, *367*, 265−272.
(23) Lee, J. R.; Won, J. H.; Kim, N. Y.; Lee, M. S.; Lee, S. Y. *J. Colloid Interface Sci.* **2011**, *362*, 607−614.
(24) Seol, J. H.; Won, J. H.; Lee, M. S.; Yoon, K. S.; Hong, Y. T.; Lee, S. Y. *J. Mater. Chem.* **2012**, *22*, 1634−1642.
(25) Xu, K.; Chanthad, C.; Gadinski, M. R.; Hickner, M. A.; Wang, Q. *ACS Appl. Mater. Interfaces* **2009**, *1*, 2573−2579.
(26) Miyatake, K.; Tombe, T.; Chikashige, Y.; Uchida, H.; Watanabe, M. *Angew. Chem.* **2007**, *119*, 6766−6769.
(27) Kwon, Y. H.; Kim, S. C.; Lee, S. Y. *Macromolecules* **2009**, *42*, 5244−5250.
(28) Ha, H. J.; Kil, E. H.; Kwon, Y. H.; Kim, J. Y.; Lee, C. K.; Lee, S. Y. *Energy Environ. Sci.* **2012**, *5*, 6491−6499.
(29) Aparicio, M.; Duran, A. *J. Sol−Gel Sci. Technol.* **2004**, *31*, 103−107.
(30) Park, Y. I.; Kim, J. D.; Nagai, M. *J. Mater. Sci. Lett.* **2000**, *19*, 2251−2253.
(31) Cho, J. H.; Park, J. H.; Lee, M. H.; Song, H. K.; Lee, S. Y. *Energy Environ. Sci.* **2012**, *5*, 7124−7131.
(32) Kalapos, T. L.; Decker, B.; Every, H. A.; Ghassemi, H.; Zawodzinski, T. A., Jr. *J. Power Sources* **2007**, *172*, 14−19.
(33) Won, J. H.; Lee, H. J.; Yoon, K. S.; Hong, Y. T.; Lee, S. Y. *Int. J. Hydrogen Energy* **2012**, *37*, 9202−9211.